Extended Data Figures and Tables

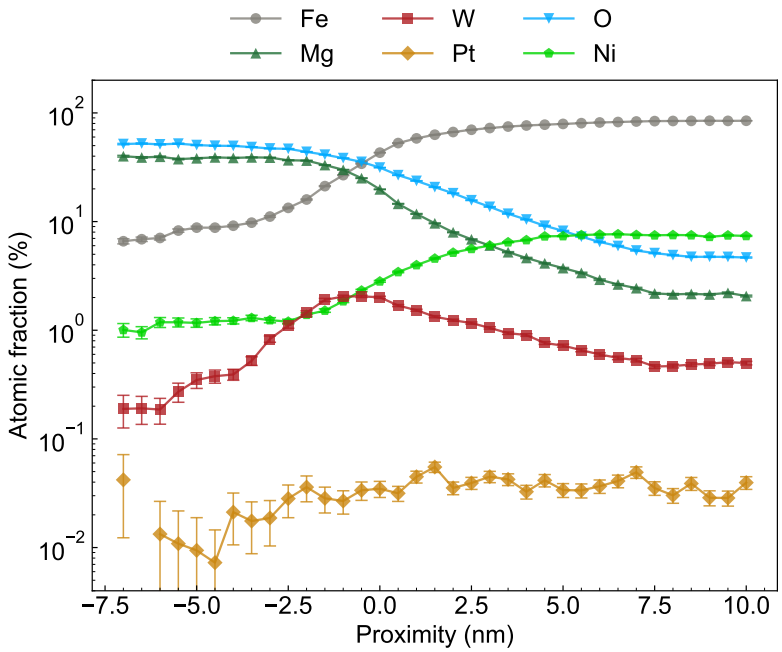

Extended Data Fig. 1 The concentration profile of various elements perpendicular to the iso-concentration surfaces of the specimen from APT analysis. The proximity is with respect to the interface of metallic melt and oxide exsolutions, determined by the intersection of the normalized concentration curves of Fe and Mg.

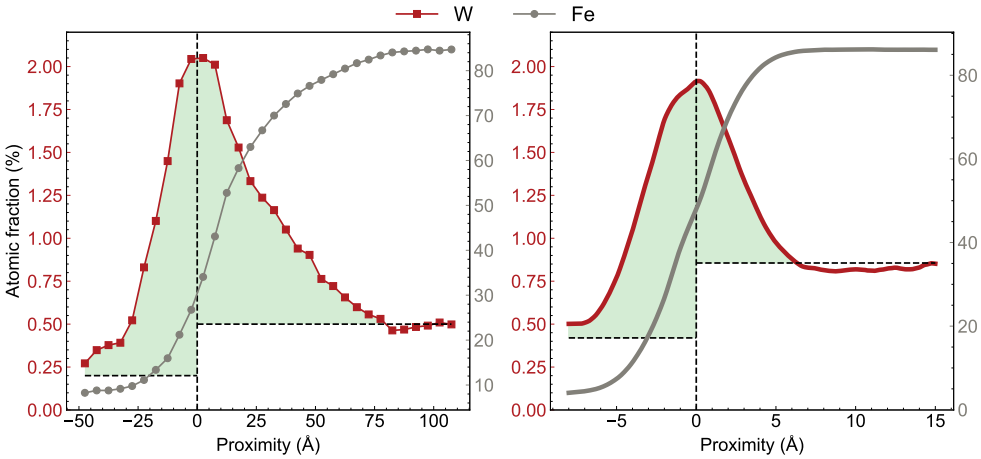

Extended Data Fig. 2 (a) The concentration profile of W perpendicular to the iso-concentration surfaces from the APT analysis (Fig. 1d). (b) The concentration profile of W perpendicular to the Gibbs dividing surface from a molecular dynamics simulation (Fig. 2a,c). The shaded region are considered as the surface excess of W. See Methods for details.

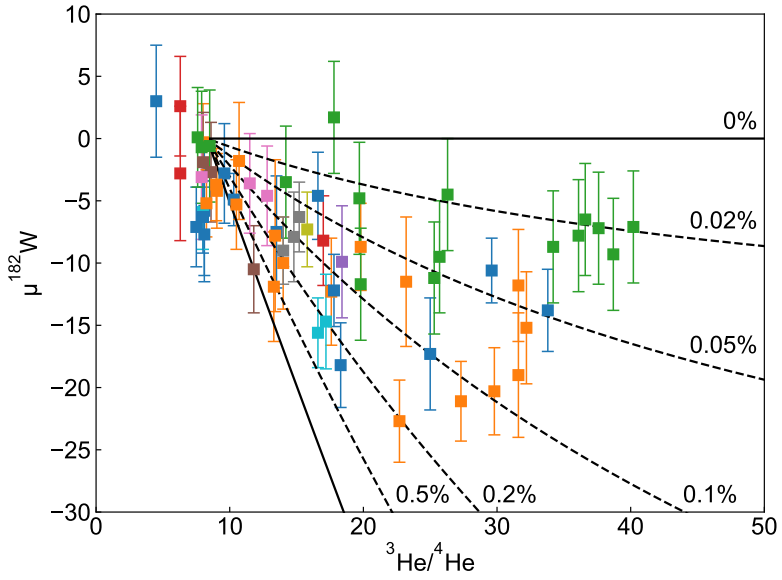

Extended Data Fig. 3 Mixing model showing correlations between $^{3}He/^{4}He$ ratios and $\mu^{182}W$ of OIB samples. Mixing between (1) ambient mantle, (2) primordial reservoir, and (3) ferropericlase exsolution. The partition coefficients of W and He at 4000 K are 0.68 (Fig. 3b) and 0.06[9], respectively. Percentages given are the proportion of ferropericlase exsolution mixed with the primordial reservoir. OIB samples compiled by ref.[5] are also shown in filled circles with 2SD uncertainties. Refer to ref.[5] and references therein for detailed discussion on the uncertainties of isotopic compositions of OIBs.

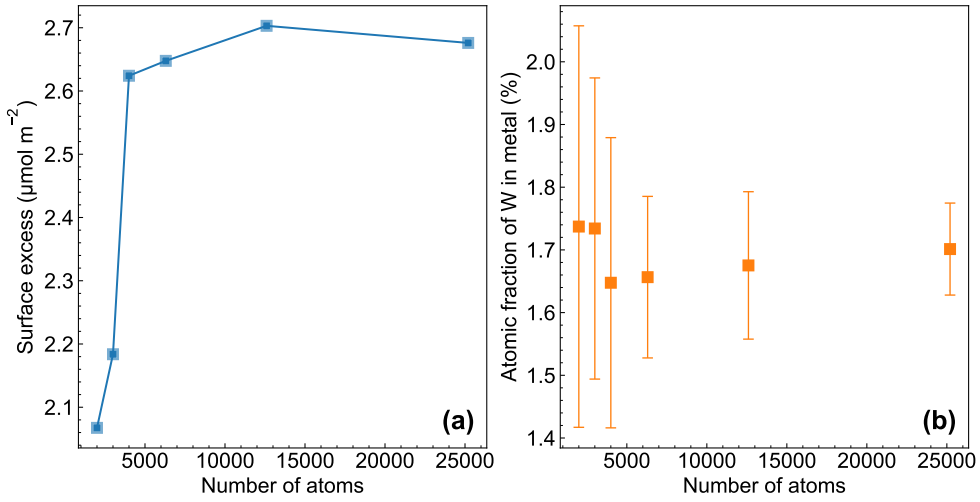

Extended Data Fig. 4 The surface excess of W (a) and concentration of W in metallic liquid (b) as a function of the number of atoms in the system after the equilibrium of oxide exsolutions under 55 GPa and 3500 K. The Mg:O:Fe:W ratio is fixed to 738:1679:3763:120 (Extended Data Table 1). The atomic fraction and surface excess converge when the system size reaches 5000 atoms.

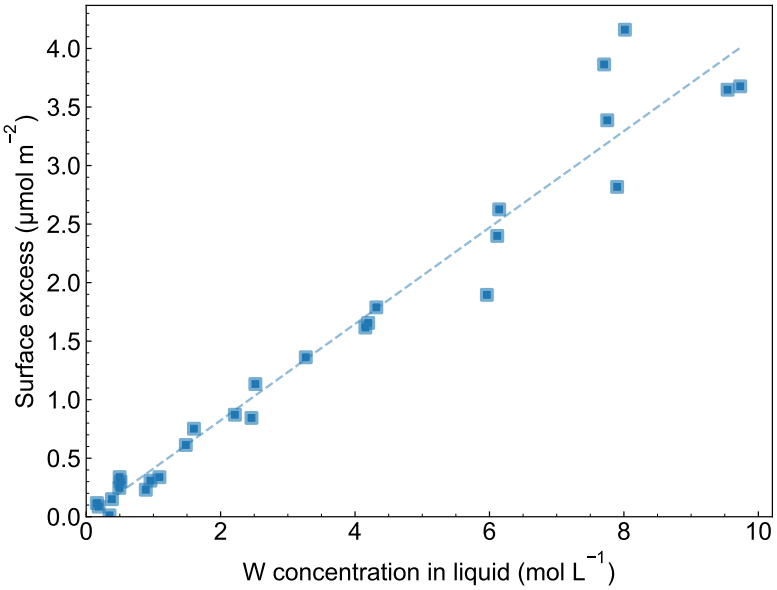

Extended Data Fig. 5 The adsorption isotherm for W on ferropericlase nanoparticles determined from 28 MD simulation runs at 4500 K and 140 GPa. The dashed line is fitted using the Henry adsorption isotherm (Eq. 11).

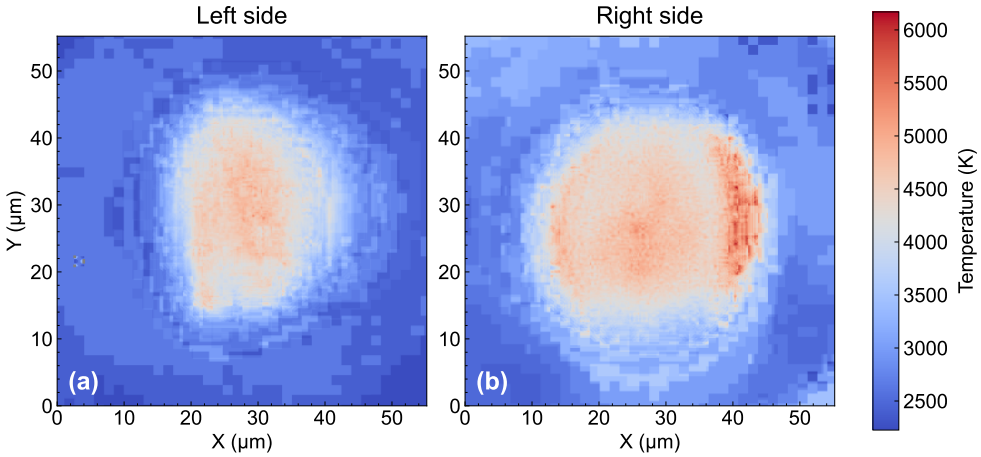

Extended Data Fig. 6 Two-dimensional temperature maps for a sample during laser heating. Note that only temperatures above 2500 K are valid for the pyrometer.

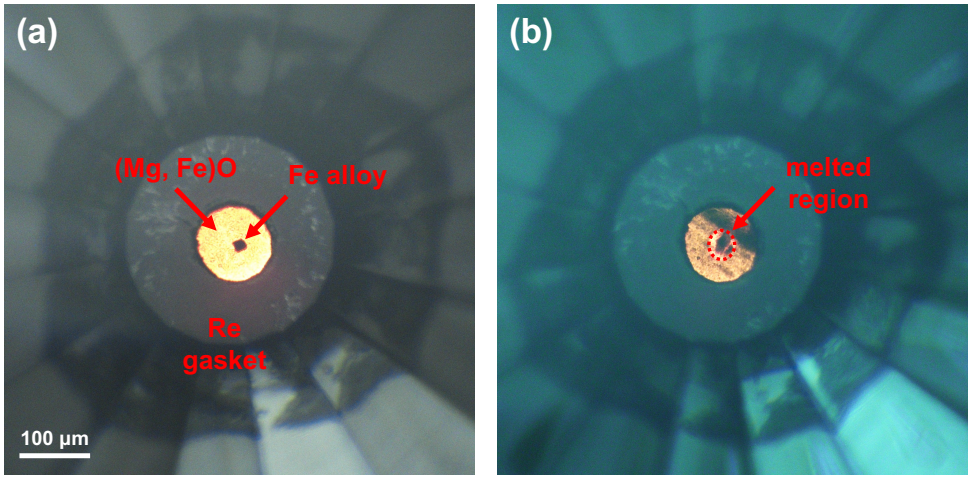

Extended Data Fig. 7 Optical image of the sample assembly at 52 GPa before laser heating (a) and quenched sample at 58 GPa (b) with transmitted and reflected light.

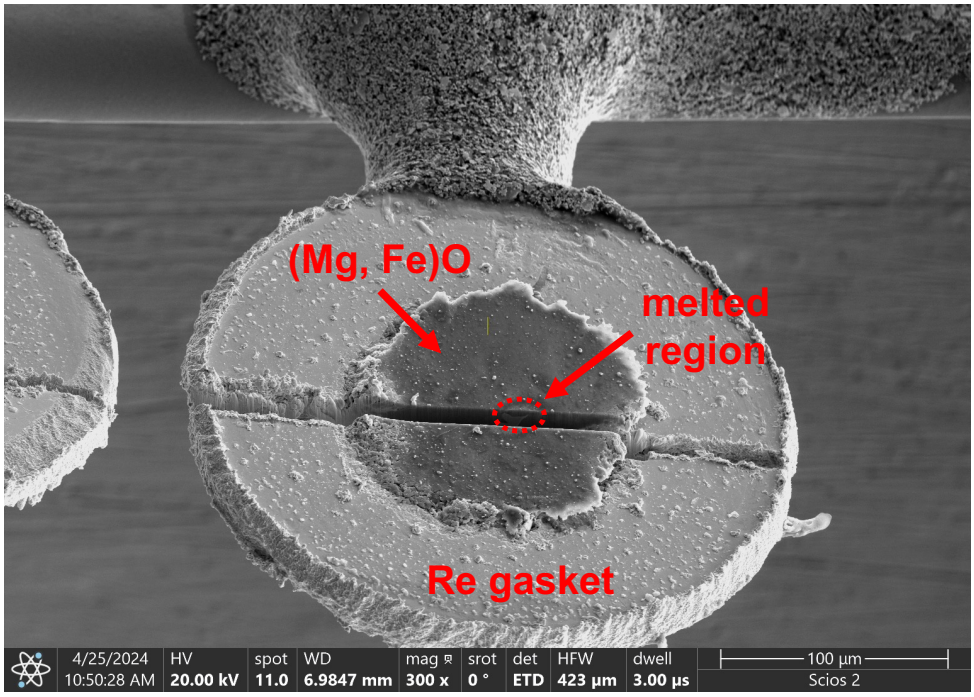

Extended Data Fig. 8 Secondary electron image of recovered sample from the laser-heating DAC experiment. The section is cut over the entire thickness of the sample and rhenium gasket to constrain the geometry of the melted region.

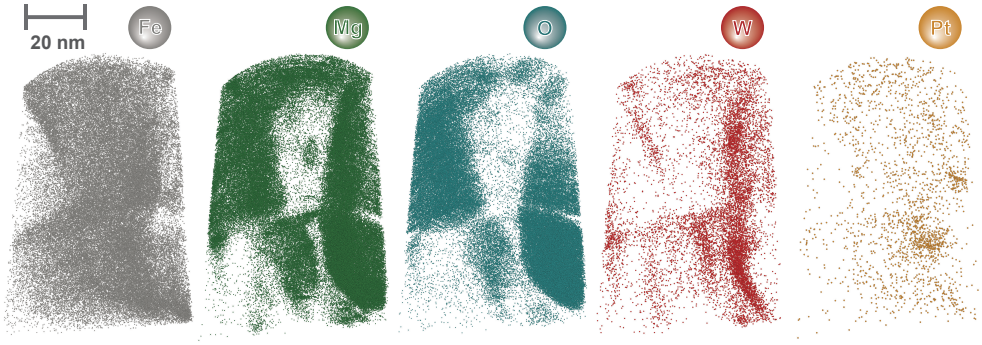

Extended Data Fig. 9 The spatial distribution of Fe (gray), Mg (green), O (blue), W (red), and Pt (yellow) in the specimen from the APT analysis.

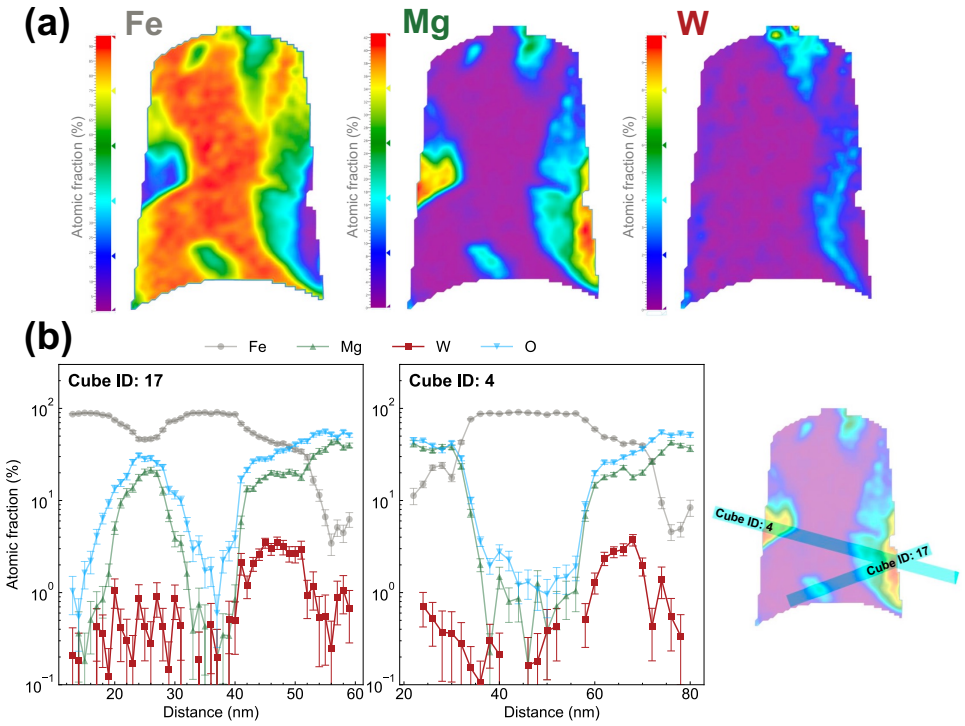

Extended Data Fig. 10 (a) Color map of the Fe (left), Mg (middle), and W (right) concentrations for a 10-nm-thick thin section from the specimen's midsection. (b) The 1D concentration profile of Fe (gray), Mg (green), W (red), and O (blue) along the long edges of two regions of interest (ROIs) of dimensions 3 × 5 × 100 nm (Cube ID: 17) and 3 × 5 × 60 nm (Cube ID: 4). The specific location of the ROIs in the specimen is shown on the right.

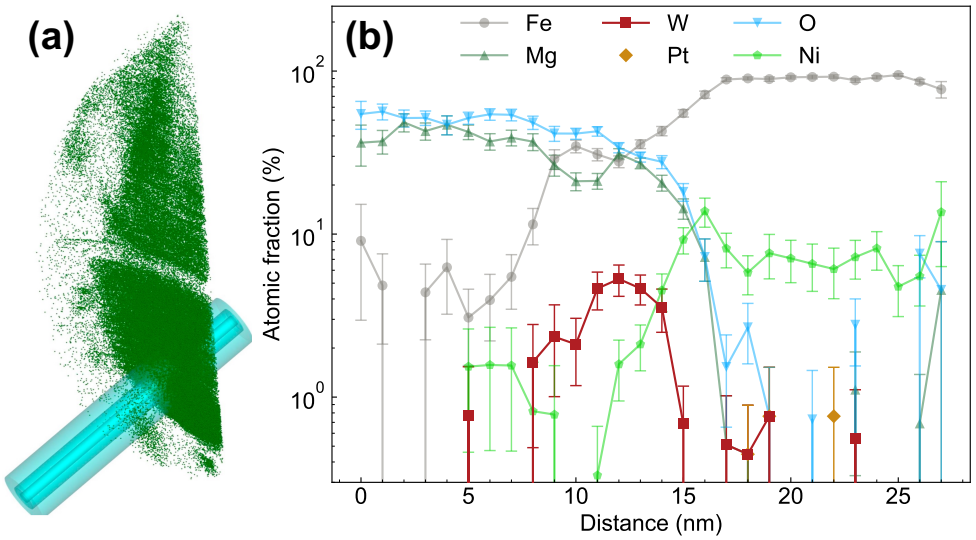

Extended Data Fig. 11 (a) A cylindrical region of interest with a diameter of 2 nm perpendicular to the relatively flat MgO boundary. The green dots represent the spacial distribution of Mg atoms. (b) The 1D concentration profile of Fe (gray), Mg (green), W (red), Pt (gold), O (blue), and Ni (light green) along the region of interest.

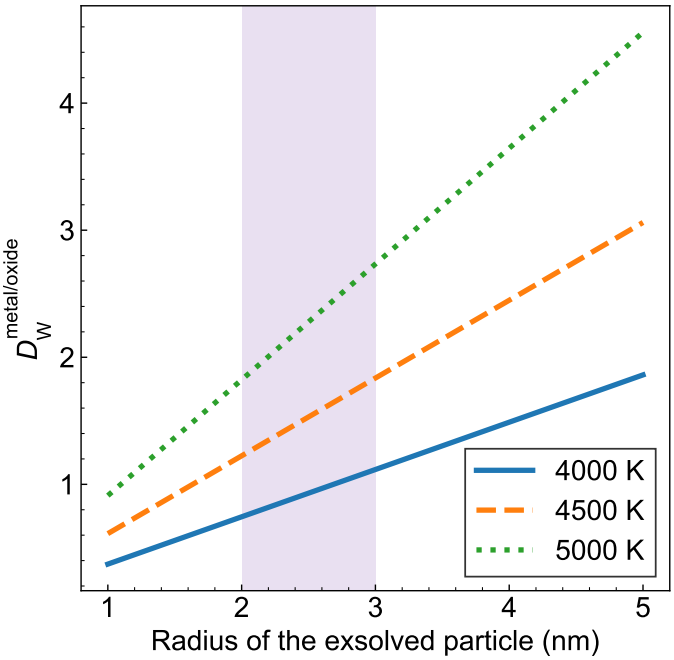

Extended Data Fig. 12 Partition coefficients between the metallic liquid and ferropericlase exsolution of W as a function of the radius of the exsolved particle at 4000, 4500, and 5000 K. The surface excess values used to calculate the partition coefficients are shown in Fig. 3.

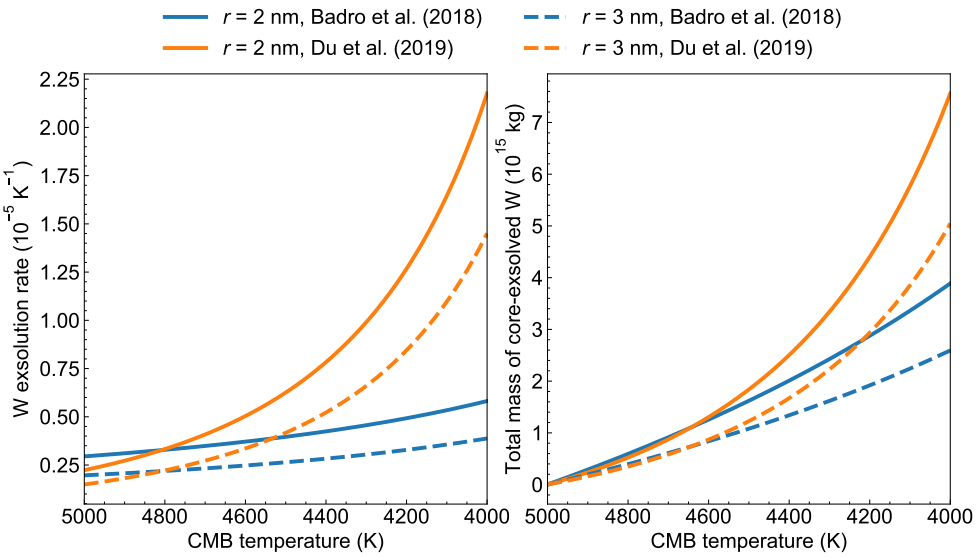

Extended Data Fig. 13 W flux transported by ferropericlase exsolution (a) and the mass of W transported into the mantle (b) as the core cools from 5000 K to 4000 K at the CMB. Orange and blue curves represent the values calculated from two MgO exsolution rates obtain by previous experiments[42,43]. Solid and dashed curves represent the values calculated from two radii of exsolution (2 nm and 3 nm, respectively).

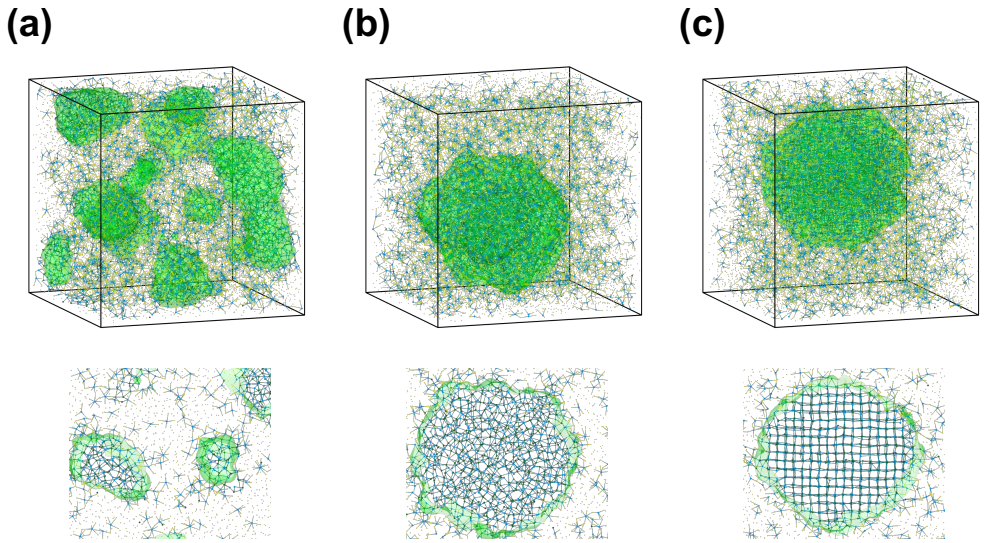

Extended Data Fig. 14 Molecular dynamics snapshots of the MgO nucleation under 4500 K and 55 GPa at 0.1 ns (a) 1.3 ns (b) and 3.7 ns (c). Mg, O and Fe atoms are colored in green, blue and yellow, respectively. The light green surface envelopes the MgO cluster in the system. The slices of the simulation boxes are shown below the snapshots. The Mg and O atoms first aggregate to form a cluster, and then homogeneous nucleation of ferropericlase occurs within the cluster.

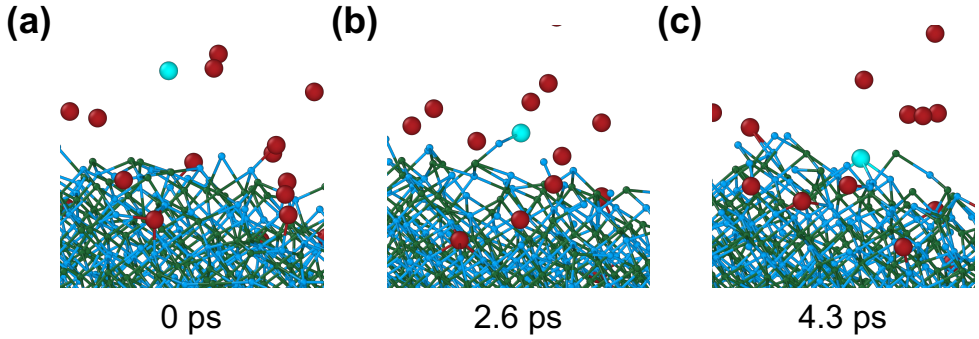

Extended Data Fig. 15 Molecular dynamics snapshots of the W adsorption on the ferropericlase surface under 4500 K and 55 GPa at 0 ps (a) 2.6 ps (b) and 4.3 ps (c). Mg, O and W atoms are colored in green, blue and red/cyan, respectively. The cyan colored W atom is tracked to demonstrate the adsorption process over the course of the simulation of 4.3 ps. Fe atoms are omitted for clarity.

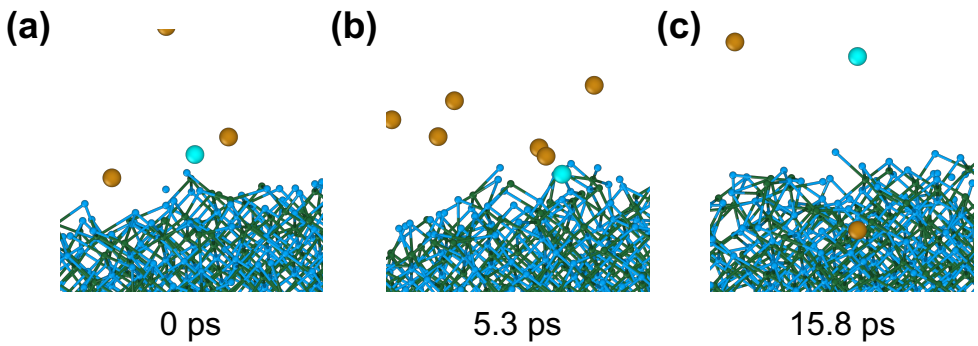

Extended Data Fig. 16 Molecular dynamics snapshots of the behavior of Pt near the ferropericlase surface under 4500 K and 55 GPa at 0 ps (a) 5.3 ps (b) and 15.8 ps (c). Mg, O and Pt atoms are colored in green, blue and gold/cyan, respectively. The cyan colored Pt atom is tracked to demonstrate the repulsion by ferropericlase over the course of the simulation of 15.8 ps. Fe atoms are omitted for clarity.

Extended Data Table 1 Pressure, temperature, and compositional conditions of all molecular dynamics simulations in this study.

Pressure (GPa)	Temperature (K)	Chemical composition				
		Mg	O	Fe	W	Pt
55	3500	234	533	1195	38	-
55	3500	351	800	1792	57	-
55	3500	469	1066	2389	76	-
55	3500	738	1679	3763	120	-
55	3500	1476	3358	7526	240	-
55	3500	2952	6716	15052	480	-
55	4500	1476	3358	7526	240	-
55	3500	1476	3358	7526	-	240
55	4500	1476	3358	7526	-	240
140	4500	1476	3358	7526	10	-
140	4500	1476	3358	7526	20	-
140	4500	1476	3358	7526	30	-
140	4500	1476	3358	7526	50	-
140	4500	1476	3358	7526	90	-
140	4500	1476	3358	7526	140	-
140	4500	1476	3358	7526	240	-
140	4500	1476	3358	7526	360	-
140	4500	1476	3358	7526	480	-
140	4500	1476	3358	7526	540	-
140	4500	1476	3358	7526	600	-
140	4500	738	1679	3763	15	-
140	4500	738	1679	3763	30	-
140	4500	738	1679	3763	60	-
140	4500	738	1679	3763	90	-
140	4500	738	1679	3763	120	-
140	4500	738	1679	3763	180	-
140	4500	738	1679	3763	240	-
140	4500	738	1679	3763	360	-
140	4000	150	931	5534	18	-
140	4000	449	931	5404	18	-
140	4000	300	931	5469	18	-
140	4000	300	1655	5262	18	-
140	4500	150	931	5534	18	-
140	4500	449	931	5404	18	-
140	4500	300	931	5469	18	-
140	4500	300	1655	5262	18	-
140	5000	150	931	5534	18	-
140	5000	449	931	5404	18	-
140	5000	300	931	5469	18	-
140	5000	300	1655	5262	18	-
140	5500	150	931	5534	18	-
140	5500	449	931	5404	18	-
140	5500	300	931	5469	18	-
140	5500	300	1655	5262	18	-
140	4000	150	207	5742	18	-
140	4000	300	207	5677	18	-
140	4000	449	207	5611	18	-
140	4000	150	931	5534	-	18
140	4000	449	931	5404	-	18
140	4000	300	931	5469	-	18
140	4000	300	1655	5262	-	18